JOURNAL OF SOLID STATE CHEMISTRY 138, 297–301 (1998)
ARTICLE NO. SC987786

Synthesis and Structural Characterization of Sr_2NbN_3 and $BaThN_2$

X. Z. Chen, Harry A. Eick,[1] and Wieslaw Lasocha[2]

Department of Chemistry and Center for Fundamental Materials Research, Michigan State University, East Lansing, Michigan 48824-1322

Received November 22, 1996; in revised form January 28, 1998; accepted February 2, 1998

Two ternary nitrides, Sr_2NbN_3 and $BaThN_2$, have been synthesized by heating under flowing N_2 at 900°C the appropriate molar mixtures of Sr_2N and NbN, and Ba_2N and Th_3N_4, respectively. The structure of Sr_2NbN_3 was refined by the Rietveld method from X-ray powder diffraction data. It crystallizes isotypically with Ba_2TaN_3 and Ba_2ZnO_3 [space group *C*2/*c* (No. 15); $a = 5.9864(2)$ Å; $b = 11.2271(3)$ Å; $c = 12.5465(1)$ Å; $\beta = 92.587(2)^\circ$, and $Z = 8$]. Based on its powder X-ray diffraction pattern $BaThN_2$ is believed to be isostructural with $BaCeN_2$ and $RbScO_2$ [space group $P6_3/mmc$ (No. 194); $a = 3.7523(6)$ Å; $c = 12.858(1)$ Å, and $Z = 2$]. Magnetic susceptibility data are consistent with the structural results. © 1998 Academic Press

Key Words: **nitride synthesis; crystal structure; Rietveld refinement; thorium; niobium; nitrogen.**

INTRODUCTION

A number of Nb- and Ta-containing nitrides have been reported: Li_7MN_4 (M = Nb (1), Ta (2)); M'_2TaN_3 (M' = Ba, Sr) (3); Ba_2NbN_3 (4); $Li_3Ba_2MN_4$ (M = Nb, Ta) (5); $CuTaN_2$ (6); $LiTa_3N_5$ (7); $Li_{2-x}Ta_{2+x}N_4$ ($\sim 0.3 < x < \sim 1$) and $Li_{1-x}Ta_{3+x}N_4$ ($x \leq 0.06$) (8); $CsNbN_2$ (9); $NaNbN_2$ (10); $TaThN_3$ (11); $Na_xTa_3N_5$ ($0 \leq x \leq 1.4$) (12); and $Li_3Sr_2MN_4$ (M = Nb, Ta) (13). In many of these compounds the similar size of Nb^V and Ta^V causes the nitrides to be isostructural. Some isostructural Nb- and Ta-containing oxonitrides are also known, e.g., $M'MO_2N$ (M' = Ca, Sr, Ba, M = Nb, Ta) (14). These close Nb–Ta similarities suggested that Sr_2NbN_3 should be preparable and isostructural with M'_2TaN_3 (M' = Ba, Sr) (3) and Ba_2NbN_3 (4). In like fashion, since Th^{IV} and Ce^{IV} have similar radii and a comparably stable oxidation state of +4, we thought $BaThN_2$ should be preparable and isostructural with $BaCeN_2$ (15). $LiThN_2$ (16), $BeThN_2$ (17), and $TaThN_3$ (11) are the only reported Th-containing ternary nitrides that we could identify.

We report the synthesis and structural studies of $BaThN_2$ and Sr_2NbN_3.

EXPERIMENTAL

Preparations were effected by placing the appropriate reactants (unless indicated otherwise) in a niobium boat which was then inserted into a quartz reaction tube through which either N_2(g) or NH_3(g) flowed. The NH_3(g) was dried over Na and stored in a stainless steel vessel. Heating schedules are indicated below. All preparations were cooled by shutting off power to the furnace. All sample manipulations were carried out in an Ar-filled glove box whose typical moisture and oxygen contents were < 0.5 ppm_v and < 1 ppm_v, respectively.

Synthesis of $BaThN_2$ and Sr_2NbN_3

Preparation of Binary Nitride Precursors

NbN. $NbCl_5$ (Johnson Matthey, grade 1) was heated under flowing NH_3 to 700°C over a three-hour period and kept at 700°C for 8 h.

Sr_2N. Sr metal (Cerac, 99%) was washed with hexane in air to remove the protective oil coating and then quickly inserted into the glove box. The oxide surface was cut away with a knife and the metal was heated in flowing N_2 at 800°C for 36 h. The observed X-ray powder pattern agreed with that calculated from the reported parameters (18).

Ba_2N. The oxide surface coating on Ba metal (Cerac, 99.7%), freed of surface oil in the glove box with Kimwipes, was cut off with a knife. The metal was heated under flowing N_2 at 870°C for 30 h. The X-ray powder diffraction pattern of the reaction product did not correspond to that of any reported Ba–N phase. We inferred the composition based on the similarity of the observed X-ray powder diffraction pattern to that of Sr_2N.

Th_3N_4. Crystals of Th metal were heated under flowing NH_3(g) at 850°C for 24 h. Observed interplanar d-spacings agreed with the reported values (19).

[1] To whom correspondence should be addressed.

[2] Present address: Department of Chemistry, Jagiellonian University, 30-060 Kraków, Poland.

0022-4596/98 $25.00

Synthesis of Ternary Nitrides

Sr_2NbN_3. Sr_2N was mixed with NbN in the molar ratio Sr : Nb = 2 : 1, heated under flowing N_2 to 900°C over a one-hour period, and held at that temperature for one day.

$BaThN_2$. Th_3N_4, mixed with either Ba_3N_2 (Cerac, 99.7%) or Ba_2N in the molar ratio Th : Ba = 1 : 1 was confined in an aluminum oxide boat. The mixture was heated slowly to 900°C under flowing N_2 and held at that temperature for 40 h.

Preliminary Phase Analysis

All products, including the binary nitride precursors, were examined first by Guinier powder X-ray diffraction with monochromatic Cu$K\alpha_1$ radiation; NBS certified Si (a = 5.43082(3) Å) was used as the internal standard. The powder pattern of Sr_2NbN_3 was indexed by comparing it with that of Sr_2TaN_3 (3). The powder pattern of $BaThN_2$ was indexed by the program DICVOL92 (20) with the hexagonal lattice parameters a = 3.7591 Å and c = 12.8749 Å. Lattice parameters were refined with the program APPLEMAN (21) Intensity calculations were performed by using the program LAZY PULVERIX (22).

Powder X-ray Diffraction Data Collection for Structural Refinement

$BaThN_2$. The nitride sample was ground thoroughly in the glove box and scattered onto a glass plate coated with double-sided Scotch tape in the glove box. A small amount of mineral oil was then spread over the sample to protect it from hydration. Intensity data were collected with a Philips APD 3720 powder diffractometer fitted with a Cu high intensity X-ray tube, a graphite monochromator, a sample spinner, and an automatic divergence slit (ADS). The diffractometer chamber was flushed continuously with nitrogen gas vaporized from $N_2(\ell)$. The Cu$K\alpha_2$ radiation component was stripped with the APD software and a correction factor was applied to convert the data to a fixed divergence slit width of 1.0° (23). The program DMPLOT (24) was used to generate a background-2θ input file.

Sr_2NbN_3. The nitride sample mixed with the Si standard was coated with mineral oil and further protected by two pieces of Scotch tape. Powder diffraction data were recorded on film using an evacuated 114.59 mm Guinier camera and Cu$K\alpha_1$ radiation. Accurate d-spacings and intensities were determined from a microdensitometric scan of the Guinier film (Zeiss Jena type 298586 densitometer modified and adapted to digital control) made at Jagiellonian University, Kraków, Poland. Background was determined as indicated above.

Rietveld Structural Refinement

The structures of both nitrides were refined with the program DBWS-9411 (25) by using the pseudoVoigt (PV) profile function. The refinement procedure for both compounds was begun with the zero correction, sample displacement, transparency factor, and scale factor parameters. The cell parameters, mixing parameters NA and NB, asymmetry factor, and half width parameters U, V, and W were included next in the refinement. After that, atomic position and isotropic temperature parameters were included. (The isotropic temperature factors of the nitrogen atoms of Sr_2NbN_3 were assigned identical values to prevent one of them from becoming nonpositive.) Finally, all of the parameters except that for sample displacement were refined together. No obvious preferred orientation effect was observed.

Since the Sr_2NbN_3 sample was contaminated with a small amount of SrO, three phases—the Si standard, SrO, and Sr_2NbN_3—were refined together. The $BaThN_2$ sample contained traces of Th_3N_4 and other unidentified impurities. Only Th_3N_4 was included as a second phase in the refinement.

Magnetic Susceptibility Measurement

Magnetic susceptibilities were measured with a Quantum Design SQUID magnetometer at temperatures between 5 and 300 K.

RESULTS AND DISCUSSION

The black $BaThN_2$ and light yellow Sr_2NbN_3 are moisture sensitive. They decompose completely to white powders within minutes on exposure to the atmosphere and release NH_3(g) which can be detected easily by moist pH paper and smell.

As expected, the powder pattern of Sr_2NbN_3 indicated it to be isostructural with Sr_2TaN_3 (3). The refinement results for Sr_2NbN_3 are shown in Table 1; the atomic positional parameters are in Table 2. The observed and calculated diffraction patterns for Sr_2NbN_3 with a difference plot indicated are shown in Fig. 1. Selected bond distances and angles are compiled in Table 3. Diffraction indices and observed and calculated interplanar distances and intensities are listed in Table 4.

Sr_2NbN_3 crystallizes isotypically with M_2TaN_3 (M = Ba, Sr) (3) and Ba_2NbN_3 (4). In this structure the Nb atoms are tetrahedrally coordinated by N atoms with an average Nb–N distance of 1.91 Å. Similar bond distances occur in Ba_2NbN_3 (4) (average Nb–N distance: 1.94 Å), $Li_3Sr_2NbN_4$ (13) (Nb–N distances vary between 1.95 and 2.00 Å), and Li_7NbN_4 (1), and $Li_3Ba_2NbN_4$ (5), both of which have average Nb–N distances of 1.95 Å, where again the Nb atoms are tetrahedrally coordinated. The average

TABLE 1
Rietveld Refinement Results for Sr_2NbN_3

Pattern 2θ range (°)	15–90
Step scan increment (2θ°)	0.015
Count time (s/step)	—
Formula weight	310.2
Space group	$C2/c$
a (Å)	5.9864(2)
b (Å)	11.2271(3)
c (Å)	12.5465(4)
β (°)	92.587(2)
Z	8
Volume (Å^3)	842.39(4)
Density (cal)(gcm^{-3})	4.891
Scale factor	4.40×10^{-5}
FWHM parameters (Half-width parameters)	
U	0.01
V	0.006
W	0.006
$R_{wp} = 100\ \{\sum w_i(y_{oi} - y_{ci})^2/\sum w_i(y_{oi})^2\}^{1/2}$	12.06
$R_p = 100 \sum \lvert y_{oi} - y_{ci}\rvert/\sum \lvert y_{oi}\rvert$	7.79

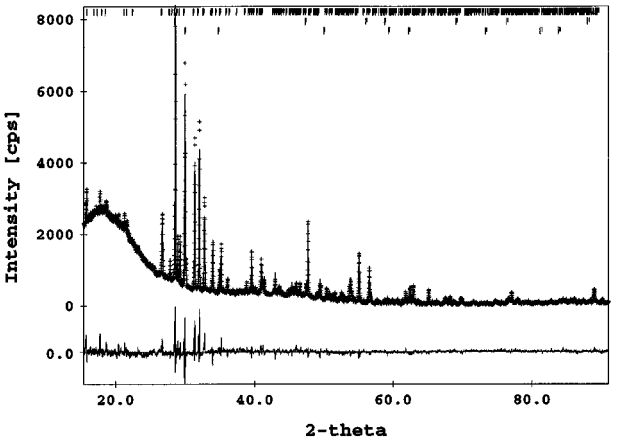

FIG. 1. A plot of the observed and calculated X-ray powder diffraction patterns for Sr_2NbN_3 with the difference plot indicated at the bottom of the figure. Two theta values of the reflections of the three phases refined (Sr_2NbN_3, Si, and SrO) are indicated at the top of the figure.

Ta–N distance in Ba_2TaN_3 (3) is 1.96 Å. The niobium–nitrogen tetrahedra are connected to each other by sharing two corners and form a one-dimensional chain $^1_\infty[NbN_{4/2}]^{6-}$ along the a direction. The coordination environments of both Sr atoms are presented in Fig. 2; the average Sr–N distance is 2.88 Å.

The refinement of the $BaThN_2$ structure gave relatively high R_p and R_{wp} factors despite numerous attempts to improve the fit. A close examination of the X-ray powder diffraction pattern indicated the presence of several weak reflections that could not be assigned to $BaThN_2$ or Th_3N_4. The principal reason for its high R factors ($R_{wp} = 14.3$, $R_p = 11.4$) is probably the poor fit of the most intense reflection at the 2θ value of about 32°. Refinements with several different peak profiles failed to improve the fit. Nevertheless, based on the similarity between the powder X-ray diffraction patterns of the Th and Ce compounds, we believe $BaThN_2$ is isostructural with $BaCeN_2$. The proposed atomic positions and the observed and calculated diffraction patterns for $BaThN_2$ with a difference plot indicated, are shown in Table 5 and Fig. 3, respectively. It crystallizes isotypically with $BaCeN_2$ (15) and β-$RbScO_2$

TABLE 2
Atomic Positions and B (eq) Values for Sr_2NbN_3

Atom	Position	x	y	z	B (Å^2)
Nb	8(f)	0.233(1)	0.0023(4)	0.3399(5)	1.4(1)
Sr(1)	8(f)	0.2726(8)	0.1142(4)	0.0771(4)	0.2(1)
Sr(2)	8(f)	0.242(1)	0.2986(4)	0.3520(5)	0.5(1)
N(1)	8(f)	0.272(6)	0.094(3)	0.464(3)	2.4(5)
N(2)	8(f)	0.334(5)	0.341(3)	0.146(3)	2.4(5)
N(3)	4(e)	0	0.062(4)	0.25	2.4(5)
N(4)	4(e)	0	0.491(4)	0.25	2.4(5)

TABLE 3
Selected Bond Distances (Å) and Angles (°) for Sr_2NbN_3

Nb–N(1)	1.87(4)	Sr(1)–N(1)	3.29(4)
Nb–N(2)	1.87(3)		2.73(4)
Nb–N(3)	1.88(2)		2.81(4)
Nb–N(4)	2.002(7)	Sr(2)–N(1)	2.69(4)
Sr(1)–N(2)	2.71(3)		2.61(4)
	2.89(4)	Sr(2)–N(2)	2.71(4)
Sr(1)–N(3)	2.83(1)		3.48(3)
Sr(1)–N(4)	2.86(2)		2.58(3)
N(2)–Sr(1)–N(2)	100.0(1.0)	Sr(2)–N(3)	3.26(4)
N(2)–Sr(1)–N(3)	131.9(6)	Sr(2)–N(4)	2.87(3)
	91.0(1.0)	N2–Sr(2)–N(2)	103.1(8)
N(2)–Sr(1)–N(1)	71.7(9)		161.0(1.0)
	70.0(1.0)		75.0(1.0)
	91.0(1.0)	N(2)–Sr(2)–N(4)	110.0(9)
	165.0(1.0)		64.1(7)
	103.6(9)		54.6(7)
N(2)–Sr(1)–N(4)	99.0(1.0)	N(2)–Sr(2)–N(1)	141.0(1.0)
	153.5(9)		99.0(1.0)
N(3)–Sr(1)–N(4)	65.8(4)		129.0(1.0)
N(3)–Sr(1)–N(1)	60.3(7)		96.0(1.0)
	103.0(1.0)		89.0(1.0)
	136.2(8)		82.0(1.0)
N(4)–Sr(1)–N(1)	121.3(7)	N(2)–Sr(2)–N(3)	72.0(7)
	88.0(1.0)		82.8(7)
	70.6(8)		125.0(8)
N(1)–Sr(1)–N(1)	83.0(1.0)	N(3)–Sr(2)–N(4)	103.4(8)
	159.0(1.0)	N(3)–Sr(2)–N(1)	61.8(9)
	79.0(1.0)		133.8(8)
		N(4)Sr(2)–N(1)	153.5(9)
			90.6(9)
		N(1)–Sr(2)–N(1)	86.0(1.0)

TABLE 4
Diffraction Indices and Observed and Calculated Interplanar Distances (Å) and Relative Intensities for Sr_2NbN_3[a]

h	k	l	d_o	d_c	I_o	I_c	h	k	l	d_o	d_c	I_o	I_c
0	0	2	6.296	6.267	4	4	2	4	1	2.0136	2.0099	9	8
0	2	0	5.624	5.614	23	15	1	5	−2	2.0081	2.0026	3	2
0	2	2	4.198	4.181	4	2	1	3	−5	1.9930	1.9901	7	4
1	1	−2	4.125	4.119	4	5	1	5	2	1.9867	1.9835	9	5
0	2	3	3.354	3.352	22	18	2	4	−2	1.9669	1.9633	12	8
1	1	−3	3.344	3.341	29	26	1	3	5	1.9485	1.9443	4	3
1	1	3	3.218	3.214	5	12	2	4	2	1.9304	1.9279	8	6
0	0	4	3.136	3.133	44	37	0	6	0	1.8738	1.8712	2	2
1	3	−1	3.098	3.093	22	21	2	4	−3	1.8633	1.8607	5	4
1	3	1	3.062	3.058	18	20	2	2	−5	1.8567	1.8548	12	12
2	0	0	2.995	2.990	100	100	0	6	1	1.8529	1.8507	4	7
1	3	−2	2.861	2.858	80	73	2	4	3	1.8241	1.8158	1	1
1	3	2	2.805	2.803	90	77	3	1	−3	1.8103	1.8077	5	7
1	1	−4		2.743		25	0	6	±2	1.7955	1.7930	4	4
			2.746		55								
0	4	±1		2.739		20	2	2	5	1.7856	1.7824	5	6
1	1	4	2.652	2.649	27	28	3	3	−1	1.7555	1.7520	6	7
0	4	±2	2.565	2.562	44	21	1	1	−7	1.7196	1.7166	9	10
1	3	3	2.502	2.498	14	8	3	3	−2	1.7148	1.7117	16	18
0	4	±3	2.333	2.330	12	5	0	6	±3	1.7108	1.7077	6	7
0	2	5	2.293	2.289	28	22	3	3	2		1.6766		16
										1.6786		31	
2	2	−3	2.277	2.273	5	5	0	4	±6		1.6758		17
1	3	−4	2.261	2.257	4	3	3	1	4	1.6376	1.6311	5	6
2	0	−4	2.217	2.214	25	18	2	4	−5	1.6096	1.6098	2	2
1	3	4	2.203	2.203	9	6	0	6	±4	1.6015	1.6065	4	2
2	2	3	2.196	2.192	12	9	2	6	0	1.5887	1.5862	2	2
2	0	4	2.120	2.116	17	14	2	6	−1	1.5806	1.5784	3	3
0	4	±4	2.095	2.091	4	2	2	6	1	1.5719	1.5690	4	7
0	0	6	2.083	2.089	4	2	2	4	5	1.5638	1.5618	2	3
1	5	−1	2.072	2.077	4	4							
2	4	−1	2.034	2.030	4	4							

[a] Intensities determined from output file of Program DBWS-9411.

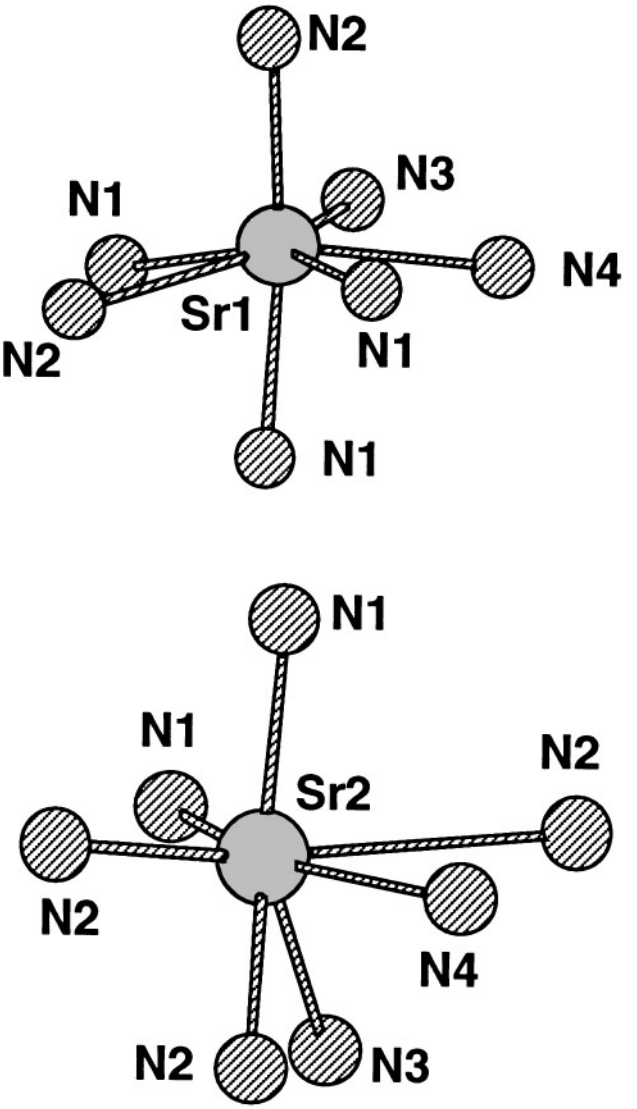

FIG. 2. The coordination environments of the two strontium atoms in Sr_2NbN_3.

(26) with the anti-TiP type structure (27). In this structure the thorium atoms are octahedrally coordinated by N atoms and each ThN_6 octahedron is connected to six other ThN_6 octahedra by edge-sharing to form a two-dimensional "octahedral" layer. Ba atoms occupy half of the trigonal prismatic holes formed by the N atoms of two adjacent octahedral layers. The N atoms are thus octahedrally coordinated by three Th and three Ba atoms in a facial arrangement.

It is interesting to speculate what, if any, other M^{IV} ions might be substituted for the Ce and Th atoms in this structure. $BaZrN_2$ crystallizes with tetragonal symmetry, space group $P4/nmm$ (4); the Zr atom is coordinated square pyramidally to nitrogen atoms. The (six-coordinate) ionic radius of Zr^{IV} is 0.27 Å shorter than that of Ce^{IV} (28), suggestive that the Zr and Hf atoms are too small to form this structure type. Thus isotypic nitrides would seem to be limited to *f*-block atoms. If oxidation is required in the synthesis of $BaMN_2$ compounds because of the choice of reagents, e.g., Ba_2N or MN_x, where the oxidation state of M is less than +4, nitrogen gas must serve as the oxidizing agent. Because it is such a poor oxidizing agent, preparation of only two other isotypic nitrides, M = Pr and U, would seem possible.

TABLE 5
Proposed Atomic Positional Parameters for $BaThN_2$

Atom	Position	x	y	z
N 4(f)	1/3		2/3	0.597(2)
Ba 2(c)	1/3		2/3	0.25
Th 2(a)	0		0	0

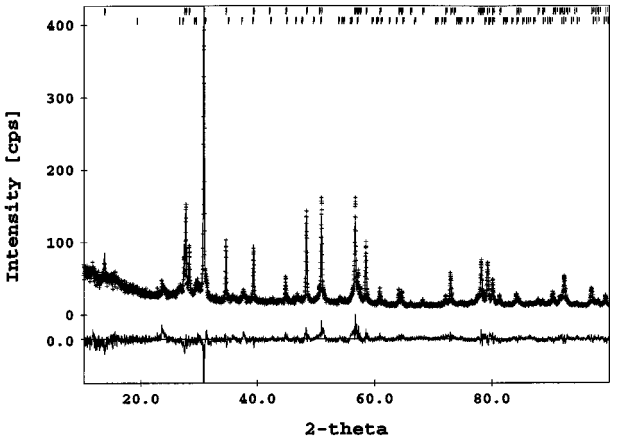

FIG. 3. A plot of the observed and calculated X-ray powder diffraction patterns for $BaThN_2$ with the difference plot indicated at the bottom of the figure. Two theta values of the reflections of the two phases refined ($BaThN_2$ and Th_3N_4) are indicated at the top of the figure.

We attempted to prepare the uranium analog by heating the appropriate stoichiometric mixtures of Ba_2N and the most-oxidized uranium nitride we could synthesize, U_2N_3, in N_2 at 950°C for 24 h and in NH_3(g) at 870°C for 48 h. In each case the powder diffraction patterns indicated in addition to reflections assignable to traces of U_2N_3 those of a new phase not isostructural with $BaThN_2$. When we substituted Sr_2N for Ba_2N, the reflections of the new phase shifted as would be expected for a smaller unit cell. We infer from these experiments that nitrogen is unable to oxidize U^{III} to the $+4$ oxidation state. For similar reasons we do not expect the $M = Pr$ analog to be preparable.

The molar magnetic susceptibility data for $BaThN_2$ show the presence of a paramagnetic impurity, probably ThN, which was not observed in the Guinier X-ray powder diffraction pattern of $BaThN_2$. However, if the weight percent of ThN in the sample were less than 4%, it would not be observed by X-ray powder diffraction. The same situation prevailed for $BaCeN_2$ due to a CeN impurity (4). Sr_2NbN_3 shows a weak temperature-independent paramagnetism between 40 and 300 K ($\chi_{average} = 3.11(8) \times 10^{-5}$ emu/mol), similar to that reported for Ba_2NbN_3 ($\chi = 1.53 \times 10^{-4}$ emu/mol) (4). At low temperature there is a Curie tail due to paramagnetic impurities.

ACKNOWLEDGMENT

The assistance of Reza Loloee in obtaining magnetic susceptibility measurements is acknowledged gratefully.

REFERENCES

1. D. A. Vennos and F. J. DiSalvo, *Acta Crystallogr.* **48,** 610–612 (1992).
2. Ch. Wachsmann and H. Jacobs, *J. Alloys Compd.* **190,** 113–116 (1992).
3. F. K.-J. Helmlinger, P. Höhn and R. Kniep, *Z. Naturforsch., B* **48,** 1015–1018 (1993).
4. O. Seeger, M. Hofmann, J. Strähle, J. P. Laval, and B. Frit, *Z. Anorg. Allg. Chem.* **620,** 2008–2013 (1994).
5. (a) X. Z. Chen and H. A. Eick, *J. Solid State Chem.* **113,** 362–366 (1994); (b) X. Z. Chen, D. L. Ward, and H. A. Eick, *J. Alloys Compd.* **206,** 129–132 (1994).
6. (a) U. Zachwieja and H. Jacobs, *Eur. J. Solid State Inorg. Chem.* **28,** 1055–1062 (1991); (b) J. M. McHale, A. Navrotsky, G. R. Kowach, V. E. Balbarin, and F. J. DiSalvo, *Chem. Mater.* **1997,** 1538–1546 (1997).
7. Th. Brokamp and H. Jacobs, *J. Alloys Compd.* **176,** 47–60 (1991).
8. Th. Brokamp and H. Jacobs, *J. Alloys Compd.* **183,** 325–344 (1992).
9. H. Jacobs and B. Hellmann, *J. Alloys Compd.* **191,** 277–278 (1993).
10. H. Jacobs and B. Hellmann, *J. Alloys Compd.* **191,** 51–52 (1993).
11. N. E. Brese and F. J. DiSalvo, *J. Solid State Chem.* **120,** 378–380 (1995).
12. S. J. Clarke and F. J. DiSalvo, *J. Solid State Chem.* **132,** 394–398 (1997).
13. X. Z. Chen and H. A. Eick, *J. Solid State Chem.* **130,** 1–8 (1997).
14. (a) R. Marchand, F. Pors, and Y. Laurent, *Rev. Int. Hautes Tempér. Réfract., Fr.* **23,** 11–15 (1986); (b) F. Pors, P. Bacher, R. Marchand, Y. Laurent, and G. Roult, *Rev. Int. Hautes Tempér. Réfract., Fr.* **24,** 239–246 (1987–1988); (c) F. Pors, R. Marchand, Y. Laurent, P. Bacher, and G. Roult, *Mater. Res. Bull.* **23,** 1447–1450 (1988).
15. O. Seeger and J. Strähle, *Z. Naturforsch., B* **49,** 1169–1174 (1994).
16. M. G. Barker and L. C. Alexander, *J. Chem. Soc. Dalton Trans.* **19,** 2166–2170 (1974).
17. V. A.-P. Palisaar and R. Juza, *Z. Anorg. Allg. Chem.* **384,** 1–11 (1971).
18. N. E. Brese and M. O'Keeffe, *J. Solid State Chem.* **87,** 134–140 (1990).
19. Powder Diffraction File, JCPDS: International Center for Diffraction Data, 1601 Park Lane, Swarthmore, PA 19081, Data 1983, File No. 24–1320.
20. A. Boultif and D. Louër, *J. Appl. Crystallogr.* **24,** 987–993 (1991).
21. D. E. Appleman, D. S. Handwerker and H. T. Evans, "Program X-ray." Geological Survey, U. S. Department of Interior, Washington, DC, 1966.
22. K. Yvon, W. Jeitschko, and E. Parthé, *J. Appl. Crystallogr.* **10,** 73–74 (1977).
23. W. Lasocha and H. A. Eick, *J. Solid State Chem.* **77,** 90–95 (1998).
24. H. Marciniak, "Plot Program DMPLOT," Version 3.2, for Viewing Results of DBWS-9006PC Rietveld Analysis Programs. Institute of Vacuum Technology OBREP, Dluga 44/50, 00-241 Warsaw, Poland, Box 386 and High Pressure Research Center UNIPRESS, Sokolowska 29/37, Warsaw, Poland.
25. R. A. Young, A. Sakthivel, T. S. Moss, and C. O. Paiva-Santos, "User's Guide to Program DBWS-9411 for Rietveld Analysis of X-ray and Neutron Powder Diffraction Patterns." School of Physics, Georgia Institute of Technology, Atlanta, GA 30332, 1994.
26. (a) R. Hoppe and H. Sabrowsky, *Z. Anorg. Allg. Chem.* **339,** 144–154 (1965); (b) H. Wiench, G. Brachtel, and R. Hoppe, *Z. Anorg. Allg. Chem.* **436,** 169–172 (1977).
27. R. W. G. Wyckoff, "Crystal Structures," Vol. 1, 2nd ed. John Wiley, New York, 1963.
28. R. D. Shannon, *Acta Crystallogr. Sect. A* **32,** 751–767 (1976).